scientific reports

Check for updates

OPEN

Enhancing breast Cancer immunotherapy using gold nanoparticles carrying tumor antigens

Mahtab Moshref Javadi[1], Neda Soleimani[1]✉ & Ashkan Zandi[2]✉

Cancer immunotherapy combined with standard treatments could provide an effective approach to enhancing anti-tumor responses. Activating antigen-presenting cells, such as dendritic cells (DCs), plays a central role in generating robust anti-tumor immune responses. Freund's adjuvant together with nanoparticles (NPs) and tumor antigens, promotes significant immune responses and shift antigen-specific T-cell activity from a Th2 to a Th1 response. Herein, Freund's adjuvant was combined with gold nanoparticles and tumor cell lysate (TCL). The AuNPs exhibited a spherical morphology. The in vitro release studies demonstrated a continuous and gradual release of AuNPs and TCL from Freund's adjuvant. The immunogenicity studies revealed high levels of cytokine secretion for IFN-γ, IL- 1, IL- 18, and TCD8+, along with reduced levels of IL- 4 cytokine in immunized mouse models in various treatment groups. In the prophylactic group, tumor growth was delayed, while in the therapeutic group, mouse models had more than 85% reduction within 31 days compared to the control group. The tumor size in the combination strategies, shrank to ~ 86% of its first size in just 17 days after treatment, while the control group tumor size increased by approximately 52%. These data suggest that the proposed drug system is an effective anti-tumor vaccine and also potentiate innate or adaptive immune responses for cancer therapy.

Keywords Breast cancer, Freund's adjuvant, Gold nanoparticles, Tumor antigens, Metronomic chemotherapy, Prophylactic

Abbreviations

CFA	Complete Freund's adjuvant
IFA	Incomplete Freund's adjuvant
AuNPs	Gold nanoparticles
TCL	Tumor cell lysate
CP	Cyclophosphamide
Th1	T helper cell type 1
Th2	T helper cell type 2
IFN-γ	Interferon gamma
IL-1	Interleukin-1
IL-4	Interleukin-4
IL-18	Interleukin-18
DCs	Dendritic cells
NK cell	Natural killer cells
SEM	Scanning electron microscope
DLS	Dynamic light scattering
UV-Vis	Ultraviolet–visible spectroscopy
EDX	Energy dispersive X-ray spectroscopy
PCR	Polymerase chain reaction
H&E	Hematoxylin& Eosin

[1]Department of Microbiology and Microbial Biotechnology, Faculty of Life Sciences and Biotechnology, Shahid Beheshti University, Tehran, Iran. [2]Nano-bioelectronic Devices Lab, Cancer Electronics Research Group, School of Electrical and Computer Eng, College of Engineering, Nano Electronic Center of Excellence, University of Tehran, P.O. Box: 14395 - 515, Tehran, Iran. ✉email: N_soleimani@sbu.ac.ir; Zandi@ut.ac.ir

DMEM	Dulbecco's Modified Eagles Medium
FBS	Fetal bovine serum
BSA	Bovine serum albumin
PBS	Phosphate-buffered saline
DEPC	Diethylpyrocarbonate
GAPDH	Glyceraldehyde-3-Phosphate Dehydrogenase
HKG	Housekeeping gene
IP	Intraperitoneal injection
OD	Optical density
NT	Nontreatment
CT	CFA-TCL
CA	CFA-AuNPs
CTA	CFA-TCL-AuNPs
CFA	TCL-AuNPs-CP: CTA-CP

Breast cancer is the most commonly diagnosed cancer in women all over the world[1]. Nowadays, severe breast cancer is not currently controlled by most conventional methods of cancer treatment (e.g. surgery, chemotherapy, hormone therapy, and radiation therapy)[2]. Conventional solid tumor therapies, on the other hand, reduce tumor size but come with a slew of drawbacks, including a low survival rate, a high chance of recurrence, and a negative impact on patients' lifestyles, etc[3]. Therefore, scientists are currently looking for alternative therapies with low side effects[4]. Among the conventional methods in cancer therapy, immunotherapy has illuminated a revolutionary way in the treatment of cancer. Immunotherapy, at the forefront of the therapeutic approach, plays a prominent role in strengthening particular immune responses against disseminated cancer cells[5]. Hence, the immune system can recognize and respond to foreign substances, including tumor antigens. Immunotherapy aims to enhance host immune responses to the tumor cells without impacting normal cells. Complementary therapies aim to naturally strengthen the body's immune system in the treatment of cancers and infections[6–9].

Various immunostimulants, so-called adjuvants, can influence the immune system by increasing immunity response. Adjuvants lead to the enhanced immunogenicity of attenuated antigens and play a critical role in increasing the persistence of immune responses and antigen-presenting cells (APCs)[10–12]. Stimulating adjuvants and immune boosters are classified into several main categories such as Nanoparticles, Mineral Salts, Bacterial Components, Oily Emulsions, Immunological Adjuvants, and Mucosal Adjuvants[13,14].

Some adjuvants can produce an antigen depot effect, which might last for weeks to months, allowing a slow and continuous release of antigens from the injection site over time[15,16]. One of the microbial products such as Complete Freund's adjuvant (CFA), is attributed to Jules Freund in the 1950 s. The Complete Freund's adjuvant, water-in-oil emulsion, is composed of heat-killed *Mycobacteria* (*M. tuberculosis*), paraffin oil, and surfactant, which is widely used to boost the immune system[17,18]. These types of adjuvants can potentially affect innate immune cells, macrophages, neutrophils, and dendritic cells. Dendritic cells are the backbone of cancer immunotherapy by producing cytokines such as IFN-α, -β, or -γ, IL- 12, and activating natural killer (NK) cells. T lymphocytes, macrophages, and NK cells are the main parts of the immune system, which infiltrate into the tumor environment and destroy cancer cells[19–22]. Incomplete Freund's adjuvant (IFA) contains, without the addition of heat-killed *mycobacteria*, the same as Complete Freund's adjuvant[23]. Incomplete Freund's adjuvant is one of the most notable types of common adjuvants in cancer vaccine trials (e.g. Melanoma, kidney carcinoma, and Multiple Sclerosis). IFA can mostly induce Th2 response. T helper 2 cells are associated with humoral immune response. Most of the studies show that Th2 responses promote tumor angiogenesis and suppress the cellular immune response against tumor cells. For instance, IL- 4 is a cytokine that is produced by Th2 cells and inhibits the function of Th1 lymphocytes, and produces IFN-γ, which ultimately provides the conditions for tumor growth[24]. Other ingredients, such as gold nanoparticles (AuNPs), have been used as antigen carriers[21]and adjuvants in vaccine candidates[25]. AuNPs are able to induce the antigen's presentation to immune cells effectively, and they can also penetrate various immune cells and activate the production of cytokines[26,27]. Gold nanoparticles (AuNPs) are widely utilized in vaccine development not only as antigen carriers but also as immunostimulatory agents. Studies have shown that AuNPs can induce tumor immunogenic cell death (ICD)[28]. ICD is a class of regulatory cell death that reactive the specific tumor immune response by release of danger signals, damage-associated molecular patterns (DAMP), from dying tumor cells[29]. Gold nanoparticles can trigger immunogenic cell death by releasing the damage-associated molecular patterns, activating dendritic cells against cancer cells, and boosting the activity of effector cells. Additionally, AuNPs can induce oxidative stress within tumor cells, further contributing to their elimination. This process that not only helps eliminate harmful cells but also supports the development of long-lasting adaptive immunity[30]. Tumor cell lysates are used to induce dendritic cell maturation and as a source for the delivery of all tumor-specific antigens. Many tumor-related antigens have been identified, and some of them are used as peptide-based vaccines for cancer immunotherapy[31].

In the present study, we researched the in vitro and in vivo effects of Freund's adjuvant along with tumor cell lysate (TCL), AuNPs, and low-dose cyclophosphamide (CP) for stimulating the immune system, and we analyzed the efficiency of these therapeutic approaches by measuring survival rates and rate of tumor shrinkage in mouse models. An oxidation-reduction procedure was used to synthesize the AuNPs, and different characterization methods, such as ultraviolet-visible spectroscopy (UV-Vis), scanning electron microscopy (SEM), and dynamic light scattering spectroscopy (DLS) were used to optimize the synthesized AuNPs. The tumor cell lysate was made by seven freeze-thaw cycles between − 196 °C and 37 °C and the concentration was determined by using nanodrop spectrophotometers. The efficiency of Freund's adjuvant in releasing AuNPs and TCL was assayed. The administered treatments were evaluated with different methods during the animal phase

study. Consecutive tumor volume measurements and body weights, real-time PCR (on spleen cells to assess the cytokines' expression), and pathological slide section (Hematoxylin and Eosin) were used to analyze the therapeutic and prophylactic effects in the mouse model groups.

Materials and methods

All experiments and methodologies in this study were approved by the Review Board and Institutional Ethical Committee of the Shahid Beheshti University, Tehran, Iran.

Cell culture

This research is an experimental-laboratory type. Triple-negative breast cancer mouse model cell line, 4T1, was purchased from the Pasture Institute of Iran (National Cell Bank of Iran). 4T1 cell tumor development and metastatic dissemination in BALB/c mouse models closely resembles human breast cancer. 4T1 cell line was cultured in the medium containing DMEM (Sigma, Germany), supplemented with 10% fetal bovine serum (FBS) (Gibco, Germany), penicillin 100 U/mL, streptomycin (Sigma, Germany) 100 µg/mL in an incubator at 37 °C and 5% CO_2. To subculture, once the cells covered at least 70% of the container, first they were detached by using 0.25% trypsin-EDTA (Gibco, Germany), and then 1×10^6 cells were transferred into new flasks.

Tumor cell lysate Preparation

The tumor cell lysate was prepared using the freeze-thaw cycle method[32]. Briefly, 4T1 cell pellets were resuspended in ice-cold phosphate-buffered saline (PBS) (Sigma, Germany), 1×10^7 cell/mL, and subjected to 7 freeze-thaw cycles of rapid freezing in liquid nitrogen (5 min) and thawing in a bain-marie at 37 °C (5 min). Then, the lysates were centrifuged at 2000 g for 10 min to remove cellular debris. The supernatant was collected and filtered using a 0.22 µm membrane filter to ensure sterilization. The protein concentration of tumor cell lysates was recognized by nanodrop spectrophotometers (Thermo ND- 2000) at 280 nm.

Synthesis and characterization of AuNPs

Before the synthesis of AuNPs, all the glassware was washed with HCl or hydrochloric acid (1%) and then washed with deionized water (DI water). Gold nanoparticles were synthesized according to the technique described elsewhere[26]. In brief, we used an oxidation-reduction reaction for the synthesis of Gold NPs[27]. Tetrachloroauric acid or $HAuCl_4$ (1%) (10 mg/ml, 500 µL) (Sigma, USA) was added to 25 ml of double-distilled water (ddH_2O) (Sigma, USA). When the solution is boiled, trisodium citrate or $Na_3C_6H_5O_7{\cdot}2H_2O$ (1%) (10 mg/ml, 3 ml) (Sigma, USA) is added to the boiling solution. After 20 min, when the color of the solution turned reddish, the solution was brought back to room temperature (25 °C) and stored at 4 °C. The size and morphology of the AuNPs were determined by ultraviolet-visible spectroscopy (UV-Vis), scanning electron microscopy (SEM), and dynamic light scattering (DLS). The zeta potential of AuNPs and AuNPs-TCL was determined by the Zetasizer Nano ZS (Malvern Instruments, UK) at 25 °C.

Freund's adjuvant release assessment

Complete Freund's adjuvant (CFA) containing 1 mg *Mycobacterium*, suspended in 0.85 ml mineral oil and 0.15 ml mono-oleate (Sigma, USA), was emulsified (1:1 (v/v)) in TCL (Group #1) and, AuNPs (Group #2). In the first step, CFA was vortexed to suspend the *Mycobacterial* particles. Then, separate syringes were used to emulsify CFA with TCL and AuNPs for nearly 10–15 min. Finally, a drop test was performed to ensure the structural integrity of the droplets. In each group (each group was divided into 7 microtubes), 100 µL of the prepared emulsion was dropped in PBS (pH 6.1) and was kept at 37 °C. For one week, the bottom layer of the solution was taken out daily and the absorbance was measured at 280 nm and 525 nm using a spectrophotometer (BioTek, US).

Preparation of animal models

For this study, seventy female BALB/c mouse models with 4 to 5 weeks and weighing approximately 19 to 20 g were purchased from the Pasture Institute of Iran and kept in laboratory animal housing under controlled and standard conditions at 22 ± 2 °C room temperature, 55 ± 2% relative humidity with a 12/12 h light-dark cycles and feeding schedule standards.

Ethical statements

All animal care and use were performed according to the guidelines of the Shahid Beheshti University Committee, Tehran, Iran under the ethical code IR.SBU.REC.1401.131. This research has been conducted in conformity with the ARRIVE (Animal Research: Reporting in Vivo Experiments) guidelines, as outlined on the official website (https://arriveguidelines.org).

Immunization protocols

For Immunization, seventy female inbred 4–5 week-old BALB/c mouse models were randomly divided into one of three treatment groups: one focusing on a prophylactic course of action, another group focusing on therapeutic treatment, and the last group utilizing a combination of the aforementioned strategies.

Tumor challenge in prophylactic group

In the prophylactic strategy, twenty female inbred 4–5 week-old- BALB/c mouse models were divided into the following treatment groups ($n = 10$): (1) Control group (PBS), (2) Prophylactic group (CFA-TCL). Mouse models were immunized twice by intra-peritoneal (IP) injections of 100 µL (the concentration of TCL was 100 µg/mouse, 1:1, (v/v)) of vaccine at days − 14 and − 7. Subsequently, the tumor challenge experiment was

performed by subcutaneously injecting 1×10^6 4 T1 cells/100 µL into the right flank on day 0 in each group, and tumor challenge with the control group was assessed.

Tumor challenge in therapeutic group

In the therapeutic strategy, forty female inbred 4–5 week-old BALB/c mouse models were divided into the four treatment groups ($n = 10$). Mouse models were injected with 1×10^6 4 T1 cells/100 µL into the right flank on day 0. Tumors appeared and were palpable ten days after injection. On days 10, 17, 24, and 31 post-tumor inoculation, mouse models were IP injected with 100 µL (the concentration of TCL and AuNPs were 100 and 50 µg/mouse, respectively, 1:1, (v/v)) of PBS (control group), CFA-TCL (group #2), CFA-AuNPs (group #3), CFA-TCL-AuNPs (group #4).

Combination of immunotherapy and chemotherapy

This group was introduced to evaluate immunotherapy combined with chemotherapy, after tumors formed, along with Freund's adjuvant and TCL-AuNPs. Cyclophosphamide (CP) was dissolved in sterile saline and given intraperitoneally following a metronomic schedule (20 mg/kg every other day) and tumor growth was compared with control and other treatment groups.

Tumor growth measurement

In each group, mouse models were monitored regularly. Tumor volume was assessed using a digital caliper with 0.01 mm accuracy, body weight by digital scales with 0.001 g accuracy, and general condition (**Table S1**, **Supplementary Information**). The tumor volume was calculated by the formula:[33]

$$\boldsymbol{Tumor\ volume}\ (\boldsymbol{mm}3) = (4/3) \times \pi \times (\boldsymbol{Length}/2) \times (\boldsymbol{Length}/2) \times (\boldsymbol{Depth}/2)$$

On days 45 and 38 in the prophylactic and therapeutic groups, respectively, five mouse models from each group were euthanized. Spleen, liver, kidney, and lungs were excised and assessed using real-time PCR to cytokine assay and histopathology. Other mouse models were all maintained in standard conditions until natural death. After the last death in each group, Kaplan–Meier curves were analyzed with the log-rank test.

Cytokine assay by real-time polymerase chain reaction (PCR)

The concentration of IL- 1, IL- 4, IL- 18, IFN-γ, and TCD8 + cytokines was assessed by real-time PCR assay, one week after the last immunization. To this end, we used five mouse models randomly. For anesthesia, 30 µL of xylazine/ketamine mixture (10 mg/kg xylazine and 90 mg/kg ketamine) was injected intraperitoneally into the mouse models. Then, they were euthanized morally by exposure to carbon dioxide (CO_2) gas, and their spleens were collected. Other mouse models were maintained under standard conditions for survival assessment. Total RNA extraction from mouse spleens was performed by TRIzol reagent (Sigma, USA) according to the manufacturer's instructions. DEPC water (Sigma, USA) was used to dissolve spleen RNA. The RNA concentration was conducted by measuring NanoDrop UV-vis spectrophotometer (Thermo ND- 2000), based on the absorbance value at 260 nm. DNase-I (RNase-free) was used to eliminate or degrade any contaminating genomic DNA. We used a reagent kit (BIOFACT Co., Ltd) including reverse transcriptase (RT) for cDNA synthesis from purified mRNAs. The cDNA was synthesized using a reagent kit (BIO FACT Co., Ltd) containing reverse-transcribed RNA enzyme. The transcription process was performed for 15 min at 37 °C, and finally, the transcription conditions were stopped for 15 s at 85 °C. Then, the polymerase chain reaction (PCR) was applied to amplify the synthesized cDNAs. Real-time PCR was performed by a thermal cycler real-time PCR System (TaKaRa, Japan). First, to break the hydrogen bonds (H-bonds) between the complementary DNA strands, the thermocycler (DNA enhancer) was set at 95 °C for 5 min to activate the DNA polymerase (DNAP) enzyme. Then 45 two-step replication cycles for 10 s at 95 °C, and then for 30 s at 60 °C were performed to increase the amount of synthesized cDNA. Finally, in order to stop the PCR reaction, the thermal cycler device was set to 75 ° C for 10 min. GAPDH as an endogenous housekeeping gene (HKG) was used to normalize the gene expression data. The alterations in the gene expression were calculated using the $2^{-\Delta\Delta CT}$ method. The sequences of primers are listed in Table 1.

Histopathology examination

Hematoxylin and Eosin (H&E) staining was done for the test and control groups on the liver, lung, kidney, and spleen. After euthanizing animals, tissues were collected and fixed in a 10% formaldehyde solution. Sections of 4 µm were made from the paraffin-embedded tissues and staining was performed following the standard procedures. All tissue sections were evaluated by optical microscopy and x100 magnification for histological changes.

Statistical analysis method

Statistical data analysis was performed by GraphPad Prism 8.0 (GraphPad Software, Inc., US), and SPSS 21.0 (SPSS, Inc., US). All data are shown as mean ± standard error. $P \leq 0.05$ was considered statistically significant.

Results

AuNPs synthesis and characterization

Gold nanoparticles were synthesized using redox reactions or an oxidation-reduction method. The synthesis of AuNPs was validated by UV-Vis, SEM, and DLS. The UV-vis absorption spectrum results in **Fig. 1-A** indicated a strong absorption spectrum at λ_{max}= 523 nm which confirms the synthesis of gold nanoparticles[34]. UV-vis spectra can be used to determine both the size and concentration of AuNPs[35]. SEM and DLS techniques were

Gene	Sequence
IL-4	F 5 ' ATCATCGGCATTTTGAACGAGGTC 3 ' R 5 'ACCTTGGAAGCCCTACAGACGA 3 '
IL-18	F 5 ' GACAGCCTGTGTTCGAGGATATG 3 ' R 5 ' TGTTCTTACAGGAGAGGGTAGAC 3 '
IL-1	F 5 ' TGGACCTTCCAGGATGAGGACA 3 ' R5 ' GTTCATCTCGGAGCCTGTAGTG 3 '
IFN-γ	F 5 'CAGCAACAGCAAGGCGAAAAAGG 3 ' R 5 'TTTCCGCTTCCTGAGGCTGGAT 3 '
CD8+	F 5 ' ACTACCAAGCCAGTGCTGCGAA 3 ' R 5 ' ATCACAGGCGAAGTCCAATCCG 3 '
GAPDH	F 5 ' CATCACTGCCACCCAGAAGACTG 3 ' R 5 ' ATGCCAGTGAGCTTCCCGTTCAG 3 '

Table 1. The List of the primers for the genes and for the GAPDH.

used as analytical tools to study the shape, size, and structure of AuNPs. SEM and DLS results shown in **Fig.** 1-**B** and **1-C** that revealed the average particle size of the synthesized gold nanoparticles is about 50–60 nm. In addition, **Fig.** 1-**D** depicts SEM-EDX analysis of the sample.

For carrying tumor cell lysate through gold nanoparticles, firstly the pH of gold nanoparticles was adjusted using 0.5 M Potassium Hydroxide (KOH) to approximately pH = 8. The tumor cell lysate was then slowly added to the AuNPs and incubated with gentle mixing for several hours. To prevent aggregation at the end of the reaction, 1% bovine serum albumin (BSA) solution was added. Following incubation, to remove any unbound antigens and excess BSA, the solution was centrifuged at 7000 rpm for 10 min. The zeta potential (ZP) of the gold nanoparticles (AuNPs) and AuNP-tumor cell lysate (TCL) complexes was measured using a Zetasizer Nano ZS (Malvern Instruments, UK). The zeta potential of AuNPs shifted from − 0.183 mV to 0.500 mV after the addition of tumor antigens. This change indicates a modification of the nanoparticle surface charge, reflecting the successful conjugation of tumor antigens to the gold nanoparticles (**Fig.** 1**E & F**).

In vitro release of tumor cell lysate and AuNPs from Freund's adjuvant

The in vitro release of tumor cell lysate (Group #1), and gold nanoparticles (Group #2), from Freund's adjuvant in phosphate buffer saline (pH 6.1) is shown in **Fig.** 2. For one week, the underlayer of each group suspension, CFA-TCL and CFA-AuNPs, was taken daily and the absorbance was measured at 280 nm and 525 nm using a spectrophotometer. The results indicate that Freund's adjuvant showed good performance in controlled release, meaning TCL and AuNPs were released slowly and continuously. The results suggest that Freund's adjuvant creates an antigen depot, which can last for weeks to months. This adjuvant is able to release the antigen slowly but continuously from the injection site causing the immune system to be exposed to antigens for a long time while also providing long-term stimulation[13,36].

Vaccination with CFA-TCL induces prophylactic antibreast cancer effects

Twenty female inbred 4–5 week old BALB/c mouse models ($n = 10$ each group) were inoculated IP with PBS (Control group), and CFA-TCL (Prophylactic group), on days − 14 and − 7. One week after the last vaccination (on day 0), 1×10^6 4 T1 cells/100 µL were injected subcutaneously for tumor challenge. Once the tumor masses were established, on day 25, treatment with CFA-TCL, was resumed, and finally, five mouse models in each group were euthanized on day 45 (**Fig.** 3-**A**).

As is clearly shown by **Fig.** 3-**B**, the control group's (PBS-treated mouse models) tumor size progressively increased following tumor inoculation, but administration of CFA-TCL exhibited a significant delay in tumor growth ($P = 0.0093$). Also, after the tumor appeared and reached a certain volume, treatment was resumed in the CFA-TCL group, on day 25. The tumor size in this group was significantly reduced compared to the control group. The body weight results are shown in **Fig.** 3-**C**, which indicates there was no significant difference in mouse models' body weights among those groups ($P = 0.5677$). The results in **Fig.** 3-**D** revealed that vaccination of CFA-TCL for inhibiting breast cancer tumors significantly increased the survival rate of this group compared to the control group ($P = 0.0024$).

Freund's adjuvant induces therapeutic antibreast cancer effects

In this group, fifty female inbred 4–5 week old BALB/c mouse models were injected with 1×10^6 4 T1 cells/100 µL into the right flank on day 0. Approximately ten days after the injection of the cancer cells, tumor growth

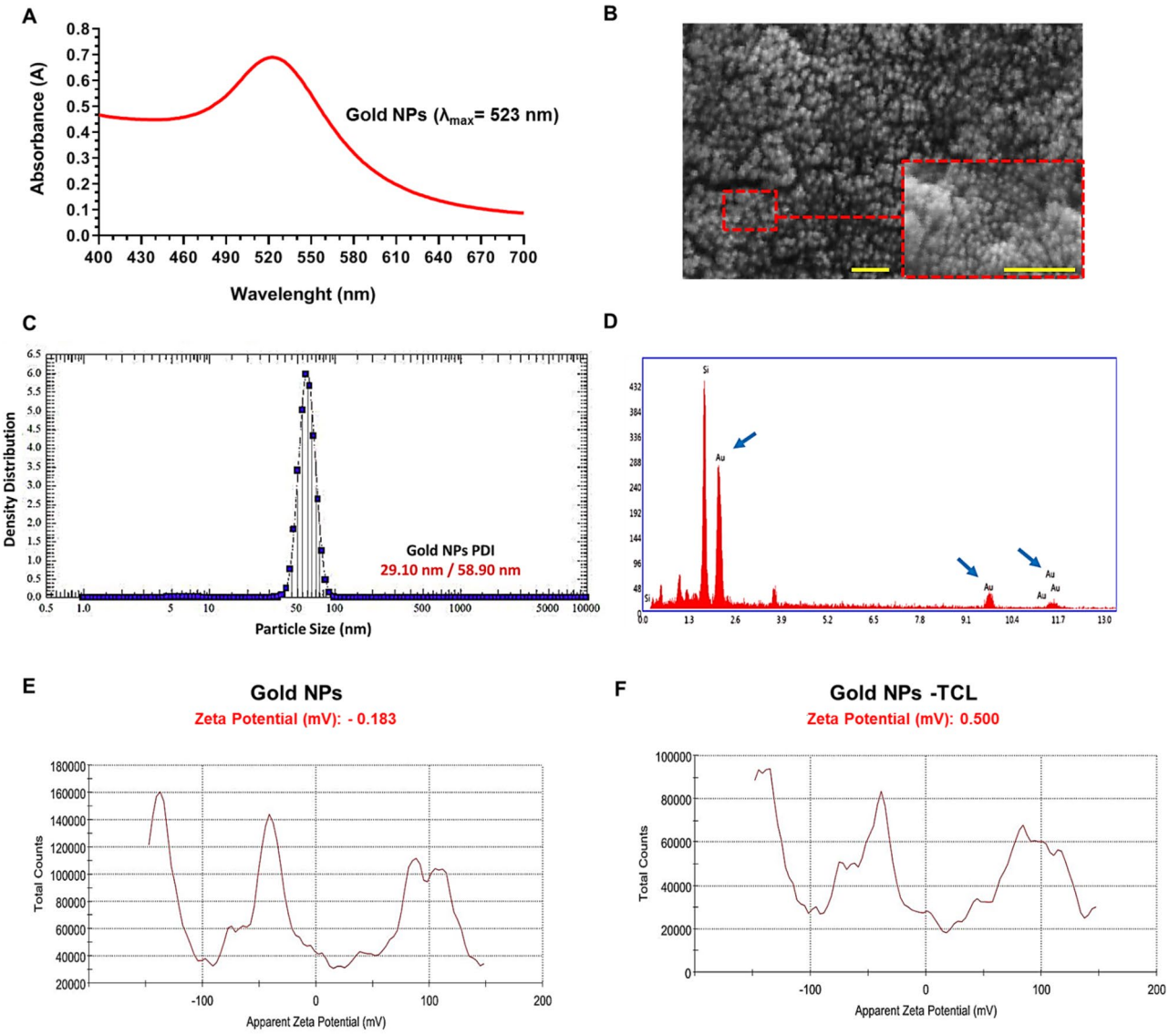

Fig. 1. **Characterization of gold nanoparticle.** (**A**) ultraviolet-visible spectroscopy (UV-Vis), (**B**) scanning electron microscopy (SEM) analysis of the particle morphology and size, (**C**) dynamic light scattering (DLS) size distribution of gold nanoparticles, (**D**) SEM-EDX analysis of the gold NPs, (**E**) Zeta potential results of Gold NPs, and (**F**) Gold NPs-TCL. As all the characterizations reveal, synthesized Gold NPs are well synthesized and well-shaped. The scale bars are set to 150 nm.

was visible, and as soon as the tumors became palpable, they were measured by caliper, and the healing process on days 10, 17, 24, and 31 post-tumor inoculation began (**Fig.** 4-**A**). The summary of all treatment groups and factors are listed in Table 2.

The results of tumor growth in the control group and the treatment groups are presented in **Fig**. 4-B. Based on the results, there is a significant difference in tumor size between the control group and the other treatment groups. As shown in **Fig**. 4-C, all of the therapeutic components significantly reduced tumor growth compared to the control group. Furthermore, the administration of CFA-TCLAuNPs-CP significantly reduced tumor growth in comparison to other groups. There was no significant difference in mouse models' body weight among those five groups (**Fig**. 4-D). Figure 4-E reveals that therapeutic components for breast cancer tumors significantly increased the survival rate; this survival rate increase in the therapeutic and prophylactic groups opens a new horizon in using Freund's adjuvant as a cancer immunotherapy approach. Another parameter indicating an enhanced immune response in treated animals was their enlarged spleen. The spleen is one of the largest immune organs, and the spleen index can be used to measure immune function[37]. **Figure** 4-F, G & H presents that the spleen size, weight, and length in mouse models exposed to treatment components increased without affecting other organs. Splenomegaly was recognized in all animals treated compared to the control group and there were no significant differences intragroup.

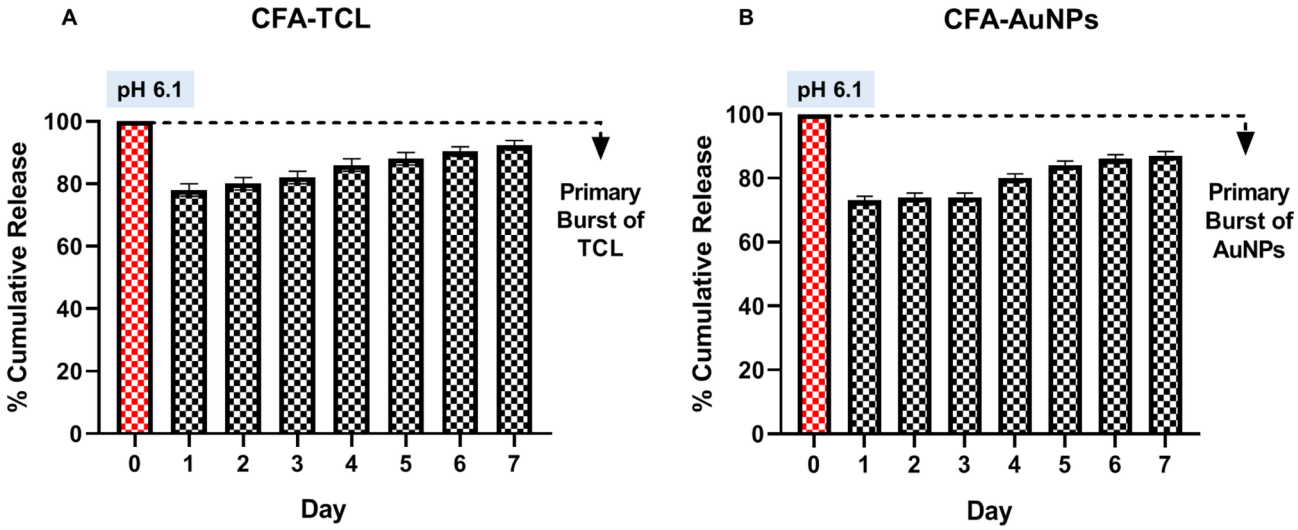

Fig. 2. **UV-Vis spectrophotometry to determine release of tumor cell lysate and AuNPs from Freund's adjuvant.** Absorption was measured at (**A**) 280 nm for tumor cell lysate and (**B**) 525 nm for AuNPs by UV-vis spectrophotometer over one week. According to these results, slow release of the CFA-TCL and CFA-AuNPs cause high stimulation and long-lasting immune responses which can be attributed to establishing an antigen depot and a slow release of antigens.

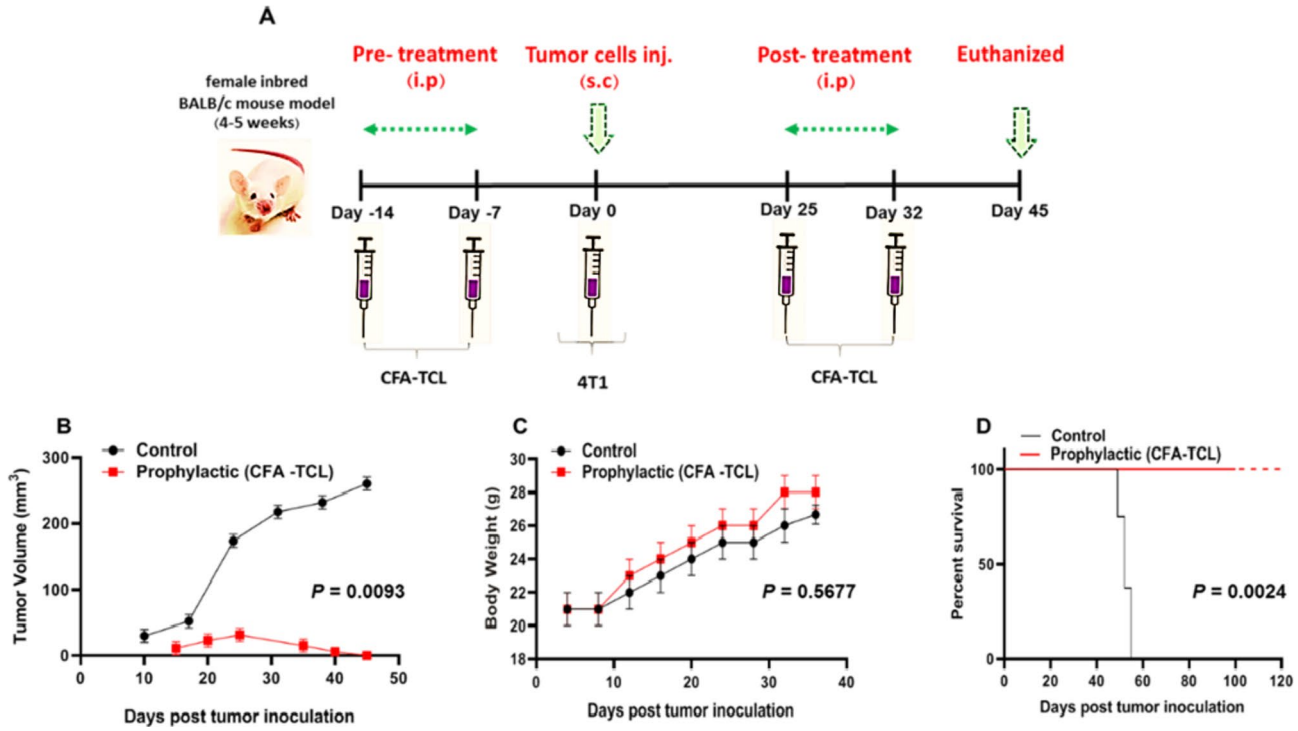

Fig. 3. **Prophylactic immunization of BALB/c mouse models with CFA-TCL**. Vaccination was performed twice in 1-week intervals. One week after the last booster, the mouse models were challenged (s.c) with 1×10^6 4 T1 cells. Mouse models vaccinated with PBS developed palpable tumors within 10 days of tumor challenge, while mouse models vaccinated with the CFA-TCL developed tumors after two weeks. This means mouse models vaccinated with CFA-TCL had the smallest tumors compared to the control group. (**A**) Schematic illustration of the experimental timeline. (**B**) In vivo evaluation of tumor growth in each group. Tumor volume was measured using calipers regularly. (**C**) Body weight of mouse models immunized with PBS, CFA-TCL. (**D**) The chart depicting survival rate of prophylactic group comparing to control group.

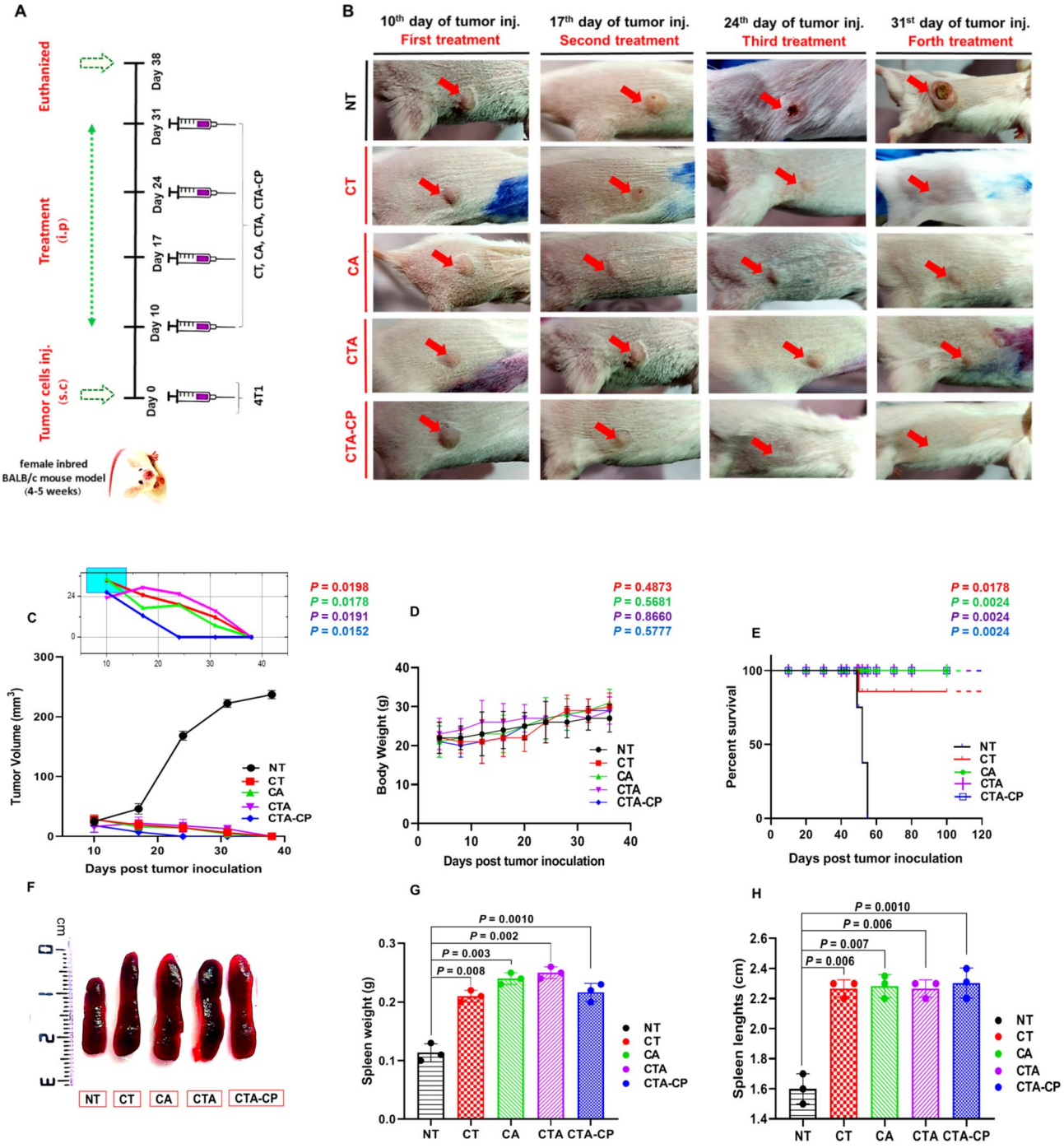

Fig. 4. **Therapeutic antitumor effect induced by CFA with TCL, AuNPs, and CP.** (**A**) Schematic representation of the experimental timeline. (**B**) Optical images of the control and treated mouse models. The tumors in the treated mouse models have been shown to be significantly reduced and destroyed. (**C**)Tumor size alterations in the five groups of the study. It is obvious that treated groups depict significant reduction in tumor size. (**D**) Body weight from mouse models immunized with PBS and therapeutic components. (**E**) The Kaplan–Meier survival curves depicting survival rate of different groups of the study (log-rank test). (**F**) The spleen size, (**G**) Spleen weights index, and (**H**) Spleen length of a control mouse and enlarged spleen of other treatment groups. This reduction in tumor size and increased spleen volume reflects stimulation of immune cells like spleen lymphocyte cause the secretion of multiple cytokines and stimulating the immune system. CT: CFA-TCL; CA: CFA-AuNPs; CTA: CFA-TCL-AuNPs; CTA-CP: CFA-CTL-AuNPs-CP.

Groups \ Factors	CFA	TCL	AuNPs	CP	Injection Intervals (Days)	Number of Injections	Treatment Time (Days)
Control	×	×	×	×	×	×	28
CT (CFA-TCL*)	✓	✓	×	×	7	4	28
CA (CFA-AuNPs**)	✓	×	✓	×	7	4	28
CTA (CFA-TCL-AuNPs)	✓	✓	✓	×	7	4	28
CTA-CP (CFA-TCL-AuNPs-CP***)	✓	✓	✓	✓	7	4	28

*** 100 µg/mouse**
**** 50 µg/mouse**
***** 20 mg/kg every other day**

Table 2. Provides a summary of all experimental groups and factors.

Measurement of cytokine levels

In order to evaluate the cell-mediated immune responses on days 45 and 38 in prophylactic and therapeutic groups, respectively, five mouse models from each group were randomly selected and euthanized. As mentioned, after RNA extraction from fresh frozen tissue and cDNA synthesis, the real-time PCR technique was employed to quantify the cytokine genes expression, including IL- 1, IL- 4, IL- 18, IFN-γ, and CD8+.

Real-time PCR results (**Fig.** 5) in prophylactic and therapeutic groups demonstrated that the expression level of all measured cytokines, except IL- 4, was higher than the control group (**Fig.** 5-**A**, **C**, **D**, **& E**), and a significant decrease in IL- 4 production was observed (**Fig.** 5-**B**), that represents switching the immune response from Th2 to Th1 response. In the prophylactic group, CFA-TCL, there was no remarkable difference in IL- 1, IL- 18, IL- 4, and CD8+ (**Fig.** 5-**A**, **B**, **C**, **& D**), while the amount of IFN-γ, in pro-CFA-TCL, raised sharply compared to other groups (**Fig.** 5-**E**).

For intergroup comparison in therapeutic groups, the amount of IL- 4, and IFN-γ did not show a significant difference **(Fig.** 5-**B**, **& E)**. Quantification of IL- 1 cytokine (**Fig.** 5-**A**) showed interleukin- 1 expressions were enhanced in all groups especially, in mouse models treated by AuNPs. In addition, the amount of CD8 + T cells in the mouse models immunized with CFA-AuNPs showed a significant change in inter and intragroup comparisons (**Fig.** 5-**D**). In **Fig.** 5-**C** in mouse models immunization with CFA-TCL shows significantly more IL- 18 production compared to the control group and other groups.

Hematoxylin and Eosin staining

The sections of excised tissue (kidney, liver, lung, spleen) of the mouse models treated by CTA-CP were stained with H&E one week after the last immunization. Comparative analyses depict no histopathological effects on mouse model organs. As shown in **Fig.** 6 no obvious malformations were observed in treated and control groups which indicates low systemic toxicity and is safe for in vivo applications.

Discussion

Although established over a century ago, cancer immunotherapy remains a revolutionary way in cancer treatment. The immune system contains several types of immune cells that have a landscape of possibilities in cancer development, progression, and clearance of tumor masses[38].

To increase the performance and immunogenicity of some antigens, it is far very beneficial to apply a few unique compounds known as adjuvants. Adjuvants can store the antigens at the injection site and this sustained release of the antigen to the antigen-presentation cells increases the immune system's response[39].

These observations describe the novel potential of complete Freund's adjuvant (CFA), combined with gold nanoparticles and tumor cell lysates, to induce an effective antitumor immune response, by intraperitoneal injection. CFA has been utilized in studies for decades, as the most well-known type of adjuvant. CFA consists of heat-killed *Mycobacteria* in mineral oil and surfactant. This adjuvant is able to emulsify in an aqueous solution, form a thick water-in-oil (W/O) emulsion, and remain in the injection site for a long time.

These findings suggest that Freund's adjuvant can be used as a powerful approach to overcome metastatic cancer due to its stimulating effects on cellular immune responses (e.g. activation of macrophages, natural killer (NK) cells, antigen-specific cytotoxic T cells). When CFA is injected intraperitoneally (IP), mycobacterial pathogen-associated molecular patterns (PAMPs) in complete Freund's adjuvant can active tumor-infiltrating antigen-presenting cells like tumor-associated macrophages (TAMs) and tumor-infiltrating dendritic cells (TIDCs)[39]. Moderate amounts of inflammation are essential for inducing and stimulating the immune system. Therefore, CFA, as a strong stimulant of the immune system, attracts inflammatory cells to the tumor site and induces anti-tumor responses[40].

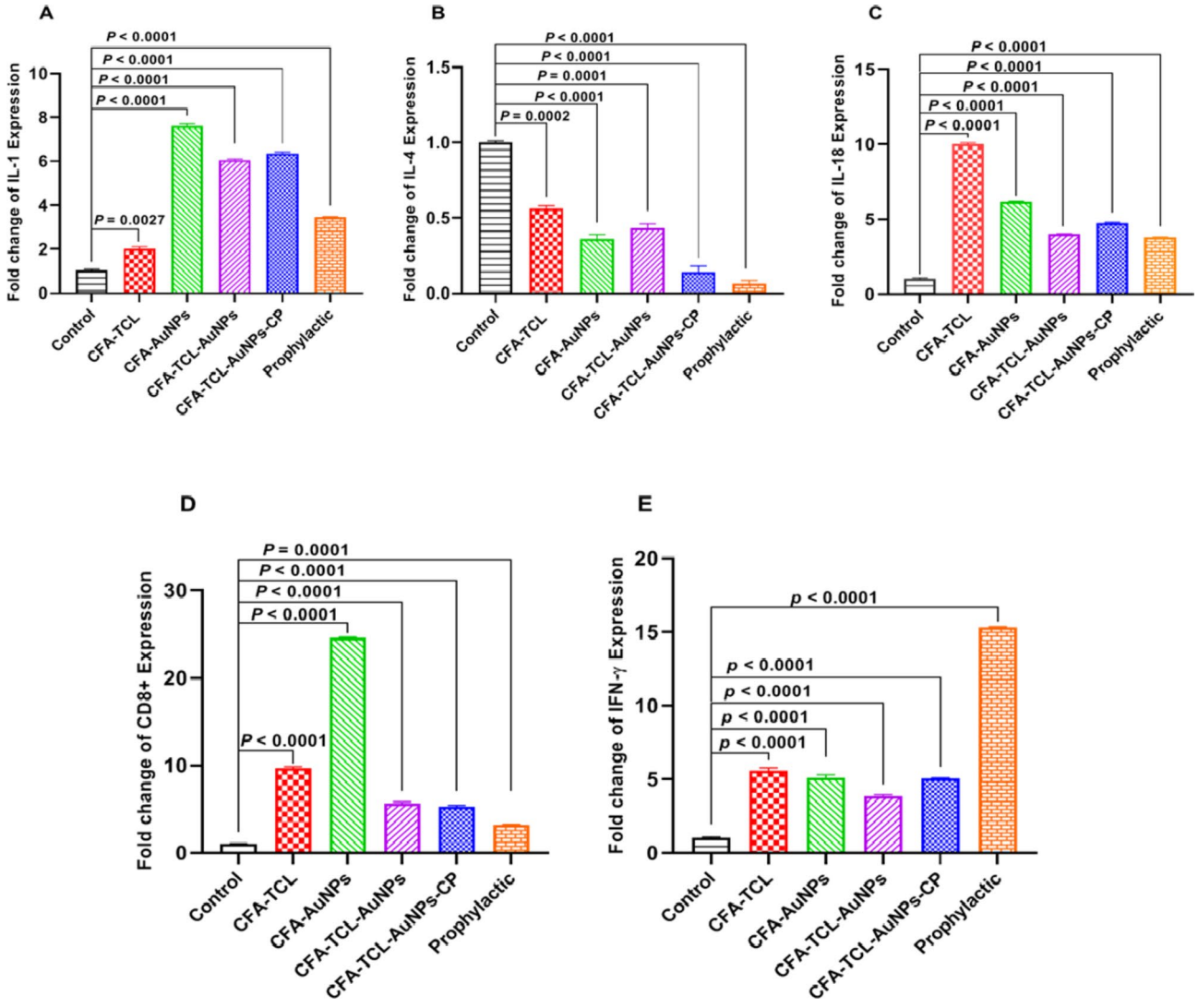

Fig. 5. **Cytokine release of mouse splenocytes stimulated by different components in therapeutic and prophylactic groups**. Level of IL- 1 (**A**),IL- 4 (**B**),IL- 18 (**C**), CD8+(**D**),and IFN-γ (**E**) secretion were analyzed in mouse splenocytes stimulated by CFA along with TCL, Au-NPs, and CP. This outcome was correlated to a reduced Th2 and Predominant Th1, as indicated by insignificant level of IFN-γ and low level of IL- 4 in all groups. Data represented the mean ± standard deviation of five mouse models per group (n = 5). Statistical analysis was perform using the t-test (GraphPad Prism8) and statistical significance was set at $p \leq 0.05$.

Judith et al.[41]concluded that vaccination with an antigen and CFA induced the secretion of antigen-specific T cells (CD4 + and CD8 + T cells). Interferon-gamma (IFN-γ) is a critical cytokine that can be used for adjuvant immunotherapy due to its anti-proliferative effects on tumors and a strong apoptosis inducer[42]. Moreover, This cytokine can inhibit tumor angiogenesis and metastatic tumors by activating CXCL10 and CXCL9[42,43].

Nagai et al.[44] showed that IFN-γ could prevent tumor cell proliferation by improving targeted therapy and increasing PD-L1 expression levels. Therefore, Freund's complete adjuvant can significantly reduce tumor size by activating IFN-γ signaling in tumor cells.

Craig L et al.[45] evaluated the effect of incomplete Freund's adjuvant (IFA) as an adjuvant in the melanoma vaccine. Administration of peptide vaccine with incomplete Freund's adjuvant can activate antitumor T cell immune responses.

Antitumor immunity involves CD4 + and CD8 + T cells. CD8 + cytotoxic T cells are well-known lymphocytic cells that can kill tumor cells through various mechanisms such as the production of TNF-α and IFN-γ. Cytotoxic CD4 + T cells can initiate antitumor immune responses by stimulating macrophages and CD8 T lymphocytes. These immune cells can identify and destroy cancer cells[46,47].

Since cytotoxic T cells can directly lysis and kill tumor cells, one of the aims of this study is to induce T-cell responses. Therefore, the type of cellular response, especially Th1, is very important to remove the tumor and create an effective immune response. In this study, all groups of mouse models treated with different compounds showed an increase in TCD8 + levels compared to the control group. Also, among the therapeutic groups, gold

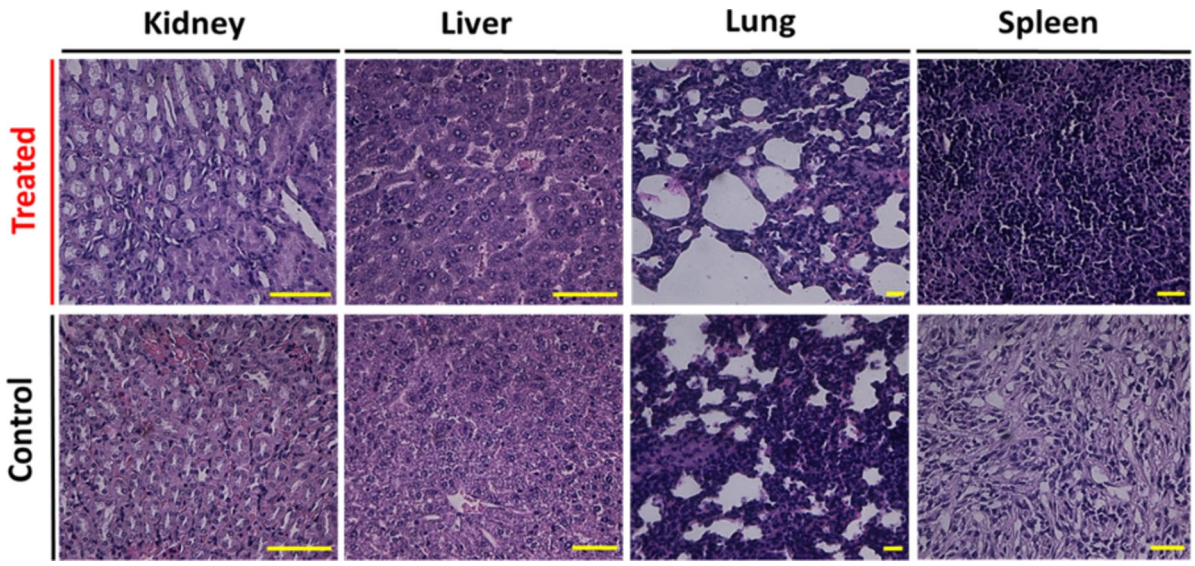

Fig. 6. **Hematoxylin and Eosin (H&E) staining results of the major organs in control and treated group**. The scale bars are set to 50 µm.

nanoparticles along with Freund's adjuvant were much more successful in inducing the TCD8 + response than other therapeutic compounds, which can be due to the effect of gold nanoparticles on immune cells, including macrophages, in stimulating TCD8 + and TCD4 + cells[48,49].

Nanoparticles have been studied for cancer therapy and vaccination as drug delivery and adjuvant, respectively. Nowadays, the use of nanoparticles has been at the center of research due to their many effects in increasing antigen processing[50,51]. Among diverse nanoparticles, gold nanoparticles are one of the excellent alternatives as nanocarriers, in accordance, with their appropriate attributes, which include non-toxicity and biocompatibility[52]. They also are capable of binding to diverse materials and antigens through strong chemical bonds (e.g. hydrophilicity-hydrophobicity, surface charge, etc.)[50]. Moreover, their synthesis and conjugation reactions are not always toxic or biologically dangerous. AuNPs induce the expression of several cytokines, including IFN-γ, IL- 8 (in both dendritic cells and macrophages), IL- 1b, and IL- 6[53]. Thus, AuNPs can penetrate various immune cells and induce the production of cytokines[53]. Considering the effects of, first, AuNPs on immune cells, induction and secretion of cytokines including; IFN-γ, TCD8+, and TCD4+, second, the impact of IFN-γ and TCD8 + on lysis and killing of cancer cells by activating dendritic cells followed by T cell proliferation and differentiation, and third, Th1 cell proliferation in cancer treatment, this study concluded that mouse groups receiving gold nanoparticles had a significant increase in TCD8 + and IFN-γ levels and also a decrease in tumor size compared to the control group. Consequently, this study suggested and used AuNPs as one of the crucial vaccine candidates.

Recently shown tumor cell lysates are used to induce dendritic cell maturation and as a source for the delivery of all tumor-specific antigens, but since the induction effect of this compound is not strong enough for dendritic cell maturation, adjuvant should be used. Many tumor-related antigens have been identified, and some of them are used clinically as peptide-based vaccines for cancer immunotherapy. These vaccine strategies primarily focus on the activity of cytotoxic TCD8 + lymphocytes, which can effectively kill tumor cells[18]. In this study, to increase the efficiency of the immune system, we combined tumor antigens with adjuvant and gold nanoparticles, in accordance, with studies on the effect of tumor antigens on immune system cells, including both dendritic cells and antigen delivery. We observed the immune system stimulation and increased cytokine secretion in different treatment groups.

These researches confirmed that there has been a remarkable correlation between the stimulatory effects of complete Freund's adjuvant and immune system response. Freund's adjuvant enhances the functional activity of lymphocytes and promotes the secretion of key anti-cancer cytokines (IFN-γ, IL- 18) without necessarily increasing their overall counts[54]. According to studies on the pivotal role of T cells and IFN-γ, pro-apoptotic and anti-proliferative effects, for tumor regression, Freund's complete adjuvant is useful to generate strong immune responses for cancer immunotherapy. Also, according to the results reported in the prophylaxis group, there was a decrease in tumor growth rate compared to the tumorized control group. Furthermore, the mouse models receiving the therapeutic compounds did not show any side effects during and after the treatment; and they were similar in weight and general condition to the tumorized control group, which indicates the biocompatibility and drug safety of the therapeutic compounds. Also, according to medical ethics, five mouse models in each group were euthanized for further evaluation and the other mouse models were kept for survival evaluation. According to the results of the study, the longevity of mouse models in the tumorized control group and different treatment groups, which is presented as the Kaplan-Meier survival curve, shows that the survival of mouse models in all treatment groups is higher than the tumorized control group and there is a significant difference between them.

An increase in survival rate would strengthen the importance of this study and the administration of these components as a promising therapeutic agent.

In this study, it was found that all therapeutic compounds reduced the size of the tumor compared to the tumorized control group; by examining the tumor size in different treatment groups, we showed that CFA with tumor cell lysate, gold nanoparticles, and anti-tumor drug cyclophosphamide, reduces tumor volume much faster than other treatment groups. Therefore, according to the mentioned results, immunotherapy as a complementary treatment along with other common treatments for cancer, including chemotherapy, plays a significant role in improving the treatment process and reducing tumor size.

Conclusion

In conclusion, we used prophylactic and therapeutic vaccines with gold nanoparticles, tumor cell lysis, and Freund's adjuvant for immunization. Nanoparticles are effective candidates for delivering tumor antigens and adjuvants to induce strong anti-tumor immunity due to their safety and adaptability. AuNPs with favorable properties, such as low cytotoxicity and the ability to improve cytokine production, could be ideal platforms. Tumor cell lysis has been used clinically in immunotherapy due to the delivery of tumor-derived antigens to dendritic cells. To enhance tumor-specific immune responses, we used Freund's adjuvant. Freund's adjuvant has an immune-stimulating effect due to the mycobacterial PAMPs, which can induce the production of Th1-stimulating cytokines from monocytes and neutrophils. This compound, with the potential to alter immune system responses, alters the phenotype from Th2 to the Th1 phenotype by producing IFN-γ. IFN-γ increases the expression of MHC class 1 and thus increases the function of TCD8 + cells, which plays an important role in cancerous tumor treatment. The antitumor role of IFN-γ has been confirmed in many studies that can inhibit tumor spread by inhibiting angiogenesis.

Stimulation of spleen cells and lymphocyte proliferation led to enlarged spleens in treatment groups and caused secretions of multiple cytokines, which, in turn, stimulated the immune systems, enhancing their ability to kill the cancer cells.

According to the results of the high-performance CFA in the gradual release model, CFA induces long-term immunity stimulation, which inhibits tumor growth.

All the results reported above show that the appearance of primary breast tumors in the prophylactic group, vaccination with TCL along with CFA, was associated with a difference of 5–9 days compared to the control group. Also, this combination significantly enhances the trend in tumor growth delay compared to the control group. A good indication of this is that after two-dose CFA-TCL, the tumor completely disappeared.

Also, in therapeutic groups, 38 days after injection with different therapeutic compounds, tumor size and growth were significantly reduced compared to the control group, and no complications were observed. Results showed that 24 days after treatment, tumors targeted by immunotherapy and metronomic cyclophosphamide, an antiproliferative drug, with at most two injections, completely disappeared. Given all this, for better performance in such areas, the combinations of other medicinal and bacterial treatments require further study.

Data availability

All data supporting the findings of this study are available within the manuscript and its supplementary information.

Received: 27 October 2024; Accepted: 3 April 2025
Published online: 14 May 2025

References

1. Venetis, K., Invernizzi, M., Sajjadi, E., Curigliano, G. & Fusco, N. Cellular immunotherapy in breast cancer: the quest for consistent biomarkers. *Cancer Treat. Rev.* **90**, 102089. https://doi.org/10.1016/j.ctrv.2020.102089 (2020).
2. Bertucci, F. et al. Genomic characterization of metastatic breast cancers. *Nature* **569**, 560–564 (2019).
3. Afzal, M. et al. in *Seminars in cancer biology.* 279–292 (Elsevier).
4. Waks, A. G. & Winer, E. P. Breast cancer treatment: a review. *Jama* **321**, 288–300 (2019).
5. Zhang, Y. & Zhang, Z. The history and advances in cancer immunotherapy: Understanding the characteristics of tumor-infiltrating immune cells and their therapeutic implications. *Cell Mol. Immunol.* **17**, 807–821 (2020).
6. Corrales, L., Matson, V., Flood, B., Spranger, S. & Gajewski, T. F. Innate immune signaling and regulation in cancer immunotherapy. *Cell Res.* **27**, 96–108 (2017).
7. Shihab, I. et al. Understanding the role of innate immune cells and identifying genes in breast cancer microenvironment. *Cancers* **12**, 2226 (2020).
8. Demaria, O. et al. Harnessing innate immunity in cancer therapy. *Nature* **574**, 45–56 (2019).
9. Huang, H. et al. The Immunomodulatory effects of endocrine therapy in breast cancer. *J. Experimental Clin. Cancer Res.* **40**, 1–16 (2021).
10. Moyer, T. J., Zmolek, A. C. & Irvine, D. J. Beyond antigens and adjuvants: formulating future vaccines. *J. Clin. Investig.* **126**, 799–808 (2016).
11. Bueno, J. Bioprospecting and their role in the innovation of vaccine adjuvants: mega diversity as a source of competitiveness. *J. Microb. Biochem. Technol.* **9**, e130 (2017).
12. Radtke, A. J. et al. Adjuvant and carrier protein-dependent T-cell priming promotes a robust antibody response against the plasmodium falciparum Pfs25 vaccine candidate. *Sci. Rep.* **7**, 1–12 (2017).
13. Apostolico, J. S., Lunardelli, V. A. S., Coirada, F. C., Boscardin, S. B. & Rosa, D. S. Adjuvants: classification, modus operandi, and licensing. *Journal of immunology research* (2016). (2016).
14. Bonam, S. R., Partidos, C. D., Halmuthur, S. K. M. & Muller, S. An overview of novel adjuvants designed for improving vaccine efficacy. *Trends Pharmacol. Sci.* **38**, 771–793 (2017).
15. Wang, Z. B. & Xu, J. Better adjuvants for better vaccines: progress in adjuvant delivery systems, modifications, and adjuvant–antigen codelivery. *Vaccines* **8**, 128 (2020).
16. Bastola, R. et al. Vaccine adjuvants: smart components to boost the immune system. *Arch. Pharm. Res.* **40**, 1238–1248 (2017).

17. Hajam, I. A., Dar, P. A., Won, G. & Lee, J. H. Bacterial ghosts as adjuvants: mechanisms and potential. *Vet. Res.* **48**, 1–13 (2017).
18. Hawksworth, D. Advancing Freund's and AddaVax adjuvant regimens using CpG oligodeoxynucleotides. *Monoclon. Antibodies Immunodiagnosis Immunotherapy*. **37**, 195–199 (2018).
19. Tong, C. W., Wu, M., Cho, W. & To, K. K. Recent advances in the treatment of breast cancer. *Front. Oncol.* **8**, 227 (2018).
20. Tom, J. K. et al. Applications of Immunomodulatory immune synergies to adjuvant discovery and vaccine development. *Trends Biotechnol.* **37**, 373–388 (2019).
21. Shi, S. et al. Vaccine adjuvants: Understanding the structure and mechanism of adjuvanticity. *Vaccine* **37**, 3167–3178 (2019).
22. Dewangan, H. K., Singh, S., Mishra, R. & Dubey, R. K. A review on application of nanoadjuvant as delivery system. *Int. J. Appl. Pharm.* **12**, 24–33 (2020).
23. Melssen, M. M. et al. A multipeptide vaccine plus toll-like receptor agonists LPS or polyiclc in combination with incomplete Freund's adjuvant in melanoma patients. *J. Immunother. Cancer*. **7**, 1–13 (2019).
24. Pollack, K. E. et al. Incomplete Freund's adjuvant reduces arginase and enhances Th1 dominance, TLR signaling and CD40 ligand expression in the vaccine site microenvironment. *J. Immunother. Cancer* **8** (2020).
25. Salazar-González, J. A., Gonzalez-Ortega, O. & Rosales-Mendoza, S. Gold nanoparticles and vaccine development. *Expert Rev. Vaccines*. **14**, 1197–1211 (2015).
26. Fytianos, K. et al. Uptake efficiency of surface modified gold nanoparticles does not correlate with functional changes and cytokine secretion in human dendritic cells in vitro. *Nanomed. Nanotechnol. Biol. Med.* **11**, 633–644 (2015).
27. Le Guével, X. et al. Nanoparticle size influences the proliferative responses of lymphocyte subpopulations. *RSC Adv.* **5**, 85305–85309 (2015).
28. Chen, X. Y., Yung, L. Y. L., Tan, P. H. & Bay, B. H. Harnessing the Immunogenic potential of gold nanoparticle-based platforms as a therapeutic strategy in breast cancer immunotherapy: A mini review. *Front. Immunol.* **13**, 865554 (2022).
29. Ma, C. et al. Nanomaterials: leading Immunogenic cell death-based cancer therapies. *Front. Immunol.* **15**, 1447817 (2024).
30. Zhou, L., Liu, H., Liu, K. & Wei, S. Gold compounds and the anticancer immune response. *Front. Pharmacol.* **12**, 739481 (2021).
31. Nowak, G., Rentzsch, O., Terzis, A. & Arnold, H. Induced hyperthermia in brain tissue: comparison between contact Nd: YAG laser system and automatically controlled high frequency current. *Acta Neurochir.* **102**, 76–81 (1990).
32. Kawahara, M. & Takaku, H. A tumor lysate is an effective vaccine antigen for the stimulation of CD4 + T-cell function and subsequent induction of antitumor immunity mediated by CD8 + T cells. *Cancer Biol. Ther.* **16**, 1616–1625 (2015).
33. Zandi, A. et al. Positive electrostatic therapy of metastatic tumors: selective induction of apoptosis in cancer cells by pure charges. *Cancer Med.* **10**, 7475–7491 (2021).
34. Nakamura, T. et al. Spectroscopic study of gold nanoparticle formation through high intensity laser irradiation of solution. *AIP Adv.* **3**, 082101 (2013).
35. Haiss, W., Thanh, N. T., Aveyard, J. & Fernig, D. G. Determination of size and concentration of gold nanoparticles from UV – Vis spectra. *Anal. Chem.* **79**, 4215–4221 (2007).
36. Awate, S., Babiuk, L. & Mutwiri, G. (Epub 2013/05/31. (2013). https://doi.org/10.3389/fimmu. 00114 PMID: 23720661, 2013).
37. Chen, C., Su, X. & Hu, Z. Immune promotive effect of bioactive peptides May be mediated by regulating the expression of SOCS1/miR–155. *Experimental Therapeutic Med.* **18**, 1850–1862 (2019).
38. Nguyen, A. T., Shiao, S. L. & McArthur, H. L. Advances in combining radiation and immunotherapy in breast cancer. *Clin. Breast. Cancer.* **21**, 143–152 (2021).
39. Warren, H., Vogel, F. & Chedid, L. Current status of immunological adjuvants. *Annu. Rev. Immunol.* **4**, 369–388 (1986).
40. Fahrer, A. M. A proposal for a simple and inexpensive therapeutic cancer vaccine. *Immunol. Cell Biol.* **90**, 310–313 (2012).
41. Gottwein, J. M. et al. Protective Anti-Helicobacter immunity is induced with aluminum hydroxide or complete Freund's adjuvant by systemic immunization. *J. Infect. Dis.* **184**, 308–314 (2001).
42. Ikeda, H., Old, L. J. & Schreiber, R. D. The roles of IFNγ in protection against tumor development and cancer immunoediting. *Cytokine Growth Factor Rev.* **13**, 95–109 (2002).
43. Ebbinghaus, C. et al. Engineered vascular-targeting antibody-interferon-γ fusion protein for cancer therapy. *Int. J. Cancer*. **116**, 304–313 (2005).
44. Nagai, Y., Tsuchiya, H., Ji, M. Q., Zhang, H. & Greene, M. I. (Am Assoc Immnol, (2017).
45. Slingluff, C. L. et al. Immunogenicity for CD8 + and CD4 + T cells of 2 formulations of an incomplete Freund's adjuvant for multipeptide melanoma vaccines. *J. Immunother.* **33**, 630–638 (2010).
46. Marzo, A. L. et al. Tumor-specific CD4 + T cells have a major post-licensing role in CTL mediated anti-tumor immunity. *J. Immunol.* **165**, 6047–6055 (2000).
47. Assudani, D. P., Horton, R. B., Mathieu, M. G., McArdle, S. E. & Rees, R. C. The role of CD4 + T cell help in cancer immunity and the formulation of novel cancer vaccines. *Cancer Immunol. Immunother.* **56**, 70–80 (2007).
48. Ferrando, R. M., Lay, L. & Polito, L. Gold nanoparticle-based platforms for vaccine development. *Drug Discovery Today: Technol.* **38**, 57–67 (2020).
49. Thakur, N., Thakur, S., Chatterjee, S., Das, J. & Sil, P. C. Nanoparticles as smart carriers for enhanced cancer immunotherapy. *Front. Chem.*, **1217** (2020).
50. Li, Y. et al. Gold nanoparticles enhance immune responses in mice against Recombinant classical swine fever virus E2 protein. *Biotechnol. Lett.* **42**, 1169–1180 (2020).
51. Chang, J. C., Diveley, J. P., Savary, J. R. & Jensen, F. C. Adjuvant activity of incomplete Freund's adjuvant. *Adv. Drug Deliv. Rev.* **32**, 173–186 (1998).
52. Kimling, J. et al. Turkevich method for gold nanoparticle synthesis revisited. *J. Phys. Chem. B.* **110**, 15700–15707 (2006).
53. Dykman, L. A. & Khlebtsov, N. G. Immunological properties of gold nanoparticles. *Chem. Sci.* **8**, 1719–1735 (2017).
54. Stils, H. F. Jr Adjuvants and antibody production: dispelling the Myths associated with Freund's complete and other adjuvants. *ILAR J.* **46**, 280–293 (2005).

Acknowledgements

Authors would like to thank Professor Mohammad Abdolahad for his instrumental advice, and the other members, Dr. S. Mousavi and Y. Kordehlachin, of Nano-Bio Electronic Lab at university of Tehran for their supports.

Author contributions

MMJ, AZ, and NS contributed to the conceptualization and conduct of research. MMJ and AZ organized the original manuscript and contributed to the preparation of figures. MMJ, AZ, and NS performed edition and reviewing. All authors carefully read the article and approved its content.

Funding statement

No funding to declare.

Competing interests
The authors declare no competing interests.

Conflict of interest
The authors declare that they have no conflict of interest.

Ethics approval
The study was conducted in accordance with of the Faculty of Life Sciences and Biotechnology, Shahid Beheshti University, Tehran, Iran principles. It was approved by the Research Ethics Committee of the Shahid Beheshti University, Tehran, Iran (code: IR.SBU.REC.1401.131). The study is reported in accordance with ARRIVE guidelines.

Additional information
Supplementary Information The online version contains supplementary material available at https://doi.org/10.1038/s41598-025-97343-2.

Correspondence and requests for materials should be addressed to N.S. or A.Z.

Reprints and permissions information is available at www.nature.com/reprints.

Publisher's note Springer Nature remains neutral with regard to jurisdictional claims in published maps and institutional affiliations.